

Electronic Supplementary Information

A microfluidic device for both on-chip dialysis protein crystallization and *in situ* X-ray diffraction

Niels Junius^{a,§}, Sofia Jaho^a, Yoann Sallaz-Damaz^a, Franck Borel^a, Jean-Baptiste Salmon^b and Monika Budayova-Spano^{a*}

a Université Grenoble Alpes, CEA, CNRS, IBS, F-38000 Grenoble, France, b CNRS, Solvay, LOF, UMR 5258, Univ. Bordeaux, F-33600 Pessac, France

*Correspondence e-mail: monika.spano@ibs.fr

§Current address: ELVESYS – Innovation Center, 1 rue Robert et Sonia Delaunay, 75011 Paris, France

Temperature control prototype

Temperature control is also often emphasized in crystallization of biological macromolecules.¹⁻⁴ Temperature is a major crystallization parameter for controlling the supersaturation and the solubility of a sample in a precise, non-invasive and reversible manner. From a thermodynamic point of view, temperature is associated with the enthalpy and entropy variations, both contributing to the free energy of the crystallization process.¹ Moreover, temperature variations can affect the quantity and quality of the crystals. For example, temperature can be used to fully or partially dissolve small crystals and then grow them back in order to acquire larger size with better shapes by removing defects.¹ The full potential of temperature as a crystallization variable is often not considered due to its difficult precise control during crystallization in conventional, macro scale setups. However, due to its significance in many biophysical processes, several microfluidic systems have been developed including the possibility of temperature control.⁵ These approaches use either external heating⁶⁻⁷ through Peltier elements or pre-heated liquids, integrated heating, as for example Joule heating or heating through chemical reaction, or heating in the bulk by using electromagnetic radiation. In this work, we chose to develop a prototype using the external heating method to control temperature for optimizing protein crystallization by using Peltier modules and copper blades, taking advantage of the simplicity and the effectiveness of this approach.

The prototype we developed for controlling temperature, allows a homogeneous adjustment of the temperature along the microfluidic chip, as well as the generation of temperature gradients depending on the application. This method relies on external heating through Peltier elements. Specifically, copper plates are used as substrate for the chip and they are thermally controlled by two Peltier modules placed on each side of the microchip along the linear fluidic channel. The first difficulty for developing and operating the system is the precision on the temperature measurement inside the protein reservoir (minimum precision of ± 0.5 K) since crystallization is a temperature sensitive and dependent process. The second difficulty was the concept of simultaneous control of various temperature values at different places on the

same chip for the investigation of different crystallization conditions and phase diagrams. We tested two different approaches. The first approach was based on using a flat copper plate, placed right beneath the microchip, supporting and covering the entire surface of the device. The second approach consisted of using two smaller copper blades, covering each a smaller portion of the chip's surface area, as shown in Figure ESI 1a. The copper blades are shown in Figure ESI 1b. The second approach allowed a more efficient and independent control over the temperature.

Figure ESI 1a is a schematic representation of the temperature control prototype. For these experiments, microchips containing 6 protein micro-reservoirs were used. Two perforated copper blades were placed underneath the chip, perpendicular to the linear fluidic channels. The copper blades were thermally controlled by two Peltier modules (Adaptive[®], Radiospares) with a size of 9 × 9 mm (2.9 W) and 12 × 25 mm (10.4 W). Type J thermocouples were placed on top of the chip to monitor the temperature on the chip generated by heating each Peltier element. The copper blades can be heated up to 50 ± 0.5 K and the J type thermocouples can operate from 223 K to 523 K. The two thermocouples were read by our LabView interface designed to control the experiments. The temperature distribution could be controlled uniformly across the chip or a gradient could be generated depending on the temperature of each Peltier module.

In order to optimize the heat transfer from the Peltier modules to the microfluidic chip, thermal paste for CPU was used. A plastic support was designed to hold all the parts, including the water cooler for extracting calories generated by one of the sides of the Peltier module, the Peltier modules, the metal blades, the temperature probes and the chip. This support was designed with SolidWorks and was made by 3D printing. A graphical interface allowed to display and record the numerical value of the different thermocouples. The thermocouples were arranged on a six-well chip and they were fixed with adhesive spread on the thermocouples' wires on the external of the measurement area, i.e. outside the protein reservoirs.

The system for the temperature control based on the copper blades makes it possible to assign a temperature on each pair of wells, belonging to a single column of the chip, independently of the two wells located next to it (Figure ESI 1a). P1 and P2 correspond to the Peltier elements and S1 and S3 are the two sensors used to read out the temperature. A graph of temperature recorded as a function of time when modifying the tension value over one Peltier module proves that temperature can be controlled with a very short delay (~ 2 min) at each side of the chip. The graph in Figure ESI 2a corresponds to the measurements with the S1 sensor and the one in Figure ESI 2b corresponds to the S2 sensor. In Figure ESI 2a, where S1 (Sensor 1) and S2 (Sensor 2) are included, it is shown that after applying a voltage of 1 V at P1, the temperature is not modified at S1. The temperature on S2 maintains its initial value, which makes it feasible to consider the independent control of the temperature of several zones of the chip. The resting temperature, when none of the Peltier modules is running, has been also drawn in dashed lines to illustrate the influence of heating or cooling from one side of the chip to the other. Due to the mechanical contact between the copper blades and the chip, deviations can be observed with regard to the resting temperature curve. The best way to

avoid these deviations is to perform preliminary tests measuring the temperature and use thermal paste until the configuration depicted in Figure ESI 2a is achieved.

This prototype for the temperature control of the crystallization of proteins has not yet been adapted to collect *in situ* X-ray diffraction data at a controlled temperature. Nevertheless, it allows the optimization of the crystallization at the microliter scale in the microfluidic chips.

The next step concerning temperature control would be to perform accurate measurements in an automated way. Thus, we conceived two methods to accomplish it. The first method is to perform simulations in order to predict a temperature map inside the protein reservoir of the chip without using a thermocouple and then calibrate the chip accordingly. The second method is to perform a feedback loop using a sensor embedded in the chip and modify Peltier power in real time through a PID (Proportional Integral Derivative) algorithm. Performing simulations enables the prediction of temperature inside the chip without the necessity to incorporate a temperature sensor, while a robust numerical model can rapidly simulate new conditions. However, when experimentally applying the predictions, the total environment of the microchip should be precisely controlled in order to correspond at the exact same conditions used to describe the theoretical model. Simple simulations were performed and validated by temperature on-chip measurements (data not shown) but this method was proven difficult to reproduce consistent results. On the contrary, using a temperature sensor permits direct feedback from the measurements and the temperature value can be adjusted in real time during the course of the experiment. This direct method has been used in the crystallization bench for temperature regulation using a PID controller.⁸ Using temperature sensors on microfluidic chips arises some limitations since the sensors have to be precisely placed on the chip area under study, which in this case is the protein reservoir, and a good thermal contact between the chip and the sensor needs to be ensured. Moreover, this method requires the development of an algorithm and a software for the input of the temperature set point. Nevertheless, the method is more robust, as shown in another application⁸ and should be considered for future developments.

Flushing time of the microfluidic channels

As the microfluidic chip is designed to explore multiple crystallization conditions in real time, we evaluated the flushing time of the channels and the volume of solution needed to switch from one crystallization condition to another. Brilliant blue FCF dye (Sigma Aldrich) with a concentration of 1 mmol L⁻¹ was used. Blue dye and water were both injected successively in the microfluidic chip at a constant pressure of 100 mbar. During the flow of the blue dye within the microfluidic channels, the molecules can diffuse through the dialysis membrane to balance the difference in concentration between the channels (containing the blue dye solution) and the protein reservoirs (being initially empty). When water was flowing within the channels, the opposite effect was observed and the blue dye escaped from the dialysis reservoir. Prior

to the experiment, the surface of the microchip was treated with air plasma in order to reduce the contact angle of the water in the protein reservoir. A piece of PDMS block was then deposited on top of the reservoir to close the assembly. The optical transparency of the PDMS allowed better visual observation of the flow as compared to the Kapton tape used during the crystallization and *in situ* X-ray diffraction experiments.

Images of the experiment were recorded at regular time intervals. In each image, two regions of the microchip, one in the reservoir and one in the channel, were selected to evaluate blue dye intensity variations in the channel/reservoir and thus to determine the reservoir flushing time. The mean intensity (a.u.) of the blue dye for the chip as a function of time is shown in Figure ESI 3, where oscillations of the blue intensity with time are observed. Figure ESI 3 shows that when water is injected into a microfluidic channel previously flushed with the blue dye solution, the average intensity of the blue dye decreases until reaching the value of zero intensity. The average characteristic flushing time of the channels was determined to be of the order of 130 s. It is interesting to compare this value to the diffusion time of the particles of the blue dye across the reservoir height (100 μm). The diffusion time can be approximately estimated by the equation: $t \approx x^2/2D$, where x is the reservoir height and D the diffusion coefficient of the blue dye in water. The diffusion coefficient (D) of the blue dye in aqueous solution was not determined experimentally. However, considering a value for D between $1 \cdot 10^{-5}$ and $9 \cdot 10^{-5} \text{ cm}^2 \text{ s}^{-1}$, we obtain values of t from 0.5 to 5 s which is far less than 130 sec.

Determination of the aqueous solution volume required to flush the microfluidic channels and exchange conditions can be done by calculating the hydrodynamic resistance of the channels. The theoretical value,⁹ neglecting the resistance from the tubings and considering rectangular channels, is approximately $4 \cdot 10^{12} \text{ Pa s m}^{-3}$. The resistance of 30 cm long tubings with 800 μm ID is $2.9 \cdot 10^{10} \text{ Pa s m}^{-3}$ and can be neglected since it represents $< 1\%$ of the total resistance. We determined that 400 μL was necessary to completely exchange the solution present in the channels by another one, for a pressure drop of 100 mbar and viscosity of 1 mPa s (i.e. the viscosity of water at 293 K). This volume seems quite high considering microfluidic applications. However, this value refers only to the volume of the crystallization solution. In particular cases where expensive solutions are used during an experiment, less than half of mL is required to switch from one condition to a new one.

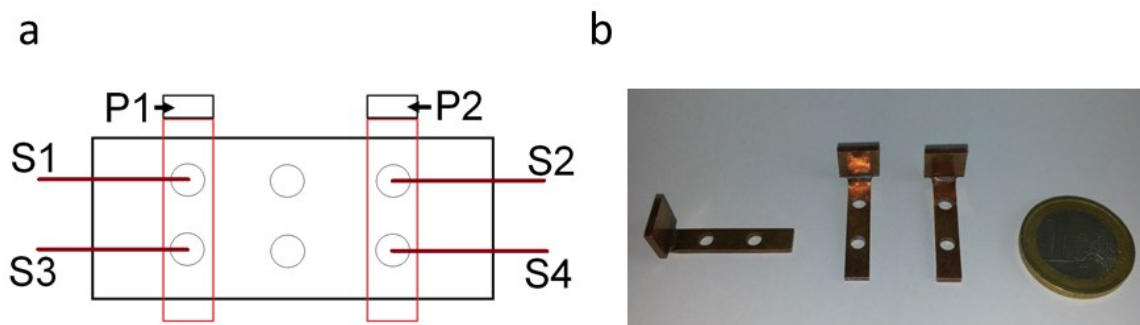


Figure ESI 1: a) Schematic representation of disposition of the Peltier modules (P1, P2) and the thermocouples (S1, S2) on the microchip containing 6 protein reservoirs. b) The copper blades designed for the temperature-controlled experiments through Peltier effect for the on-chip protein crystallization.

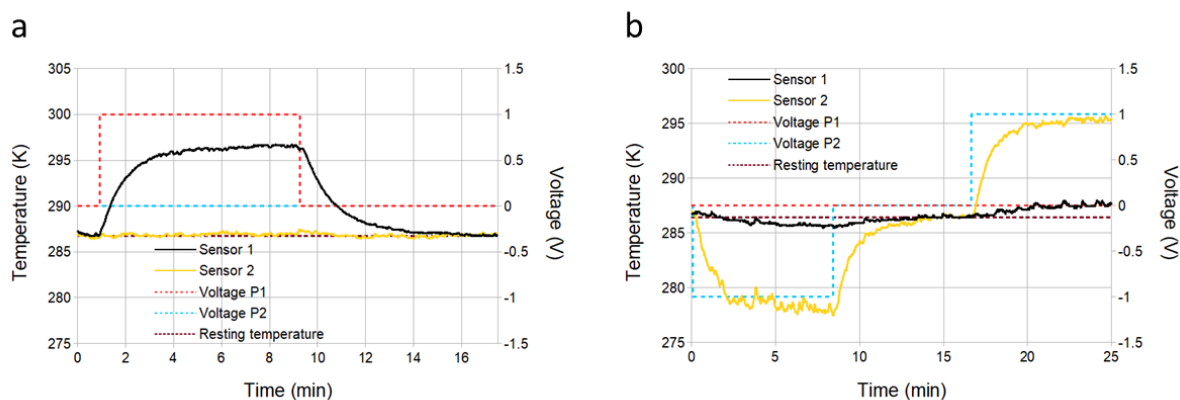


Figure ESI 2: a) Temperature variations over time on thermocouples S1 and S2 when the tension on P1 Peltier module is modified. b) Temperature variations over time on thermocouples S1 and S2 when the tension on P2 Peltier module is modified.

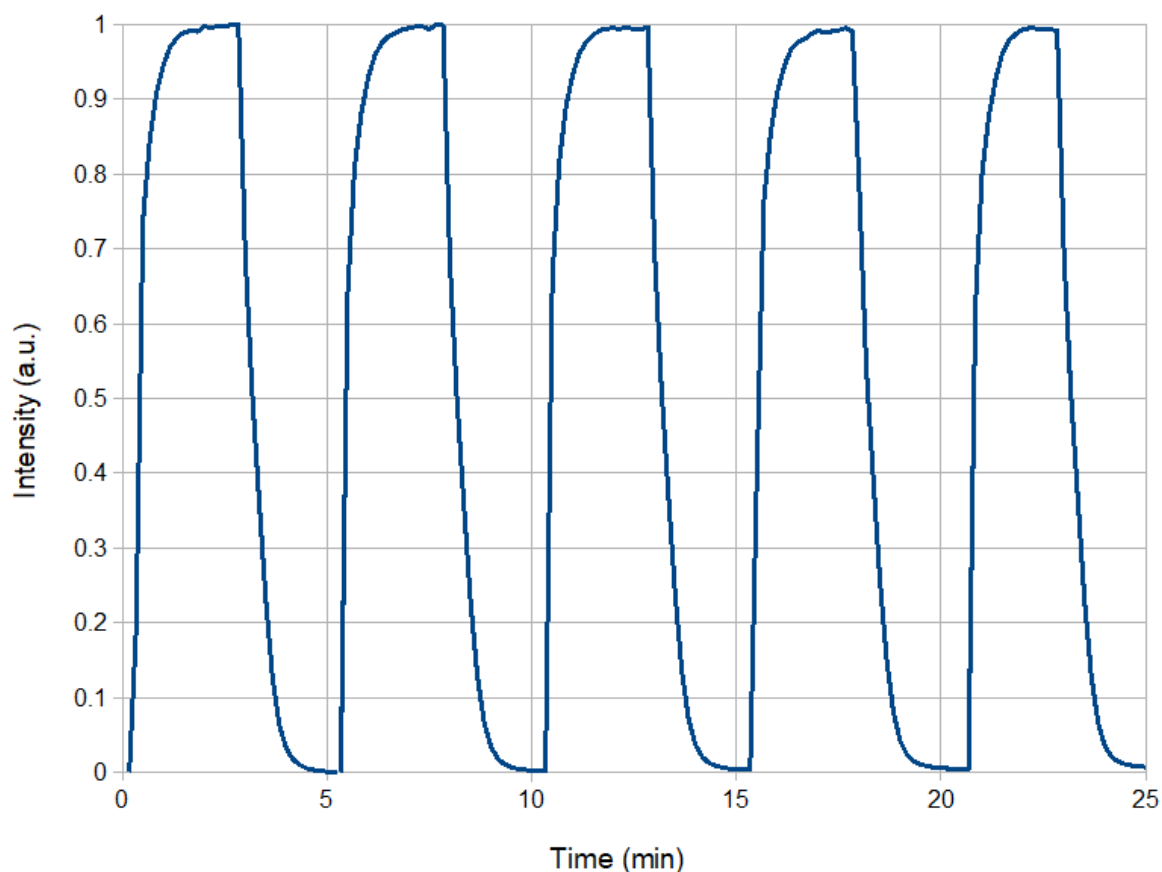


Figure ESI 3: Normalized mean intensity of the blue dye solution as a function of time, while switching the solutions within the microfluidic channels from blue dye to water and so on.

***In situ* X-ray diffraction experiments**

The microchips were mounted in front of the X-ray beam using the robotic arm G-Rob and a sample support that we designed for these experiments. This robotic arm is designed to be used in beamlines dedicated to macromolecular crystallography for mounting protein crystals on cryoloops or crystals grown in traditional 96-well crystallization plates compatible with *in situ* X-ray diffraction experiments. The support is shown in Figure ESI 4 and it can carry up to 3 microchips simultaneously. It enables data collection with an angular range of -35° to $+35^{\circ}$ around the crystal rotation. The dimensions of the holder are the same as the dimensions of commercial crystallization plates (96wells/SBS standard). In Figure ESI 4, the support for the microchips is shown in comparison to a CrystalQuickX plate (Figure ESI 4b). The support was designed with SolidWorks and was printed using 3D printing. The design and use of the microchips' support contributes to the automation of the whole process (from on-chip protein crystallization to *in situ* X-ray diffraction measurements), since no manual handling or harvesting of the crystals is required, reducing their potential damage. Figure ESI 4c illustrates 3 microfluidic chips on the 3D printed support as they were mounted by the robotic arm in front of the X-ray beam at BM30A-FIP during the *in situ* X-ray diffraction measurements.

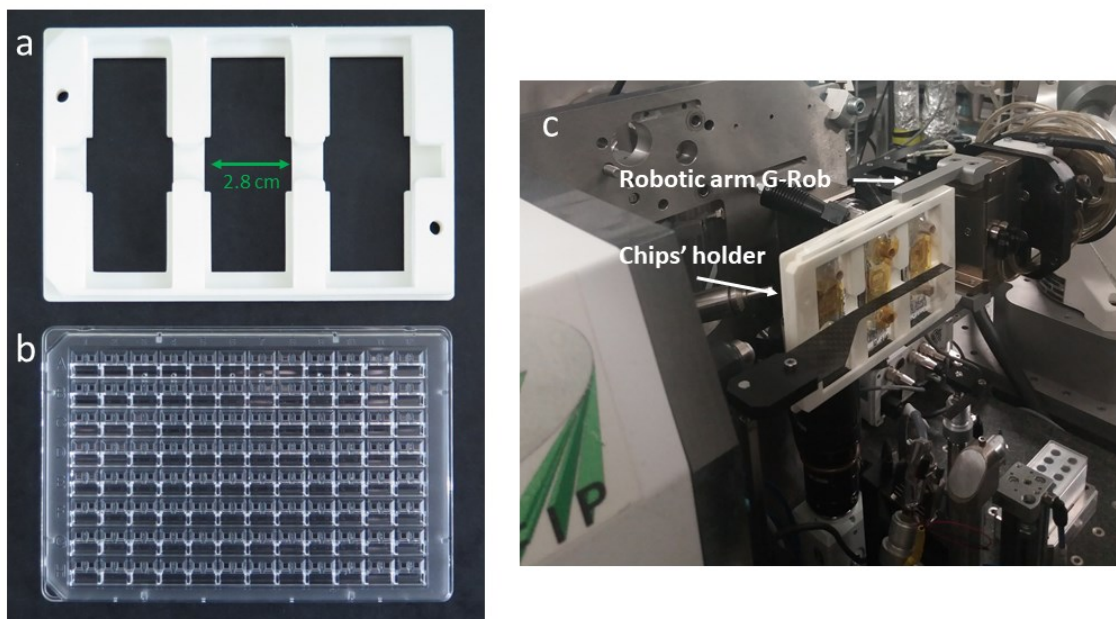


Figure ESI 4: Comparison between the 3D printed support for microchips (a), adapted to carry chips in front of the X-ray beam, and a CrystalQuickX crystallization plate (b). Up to 3 microchips can be carried by the 3D printed support and be mounted in any beamline facility suitable for *in situ* and in plate data collection. For our experiments, the *in situ* X-ray diffraction measurements were carried out at BM30A-FIP (ESRF) equipped with a robotic arm for the mounting of the microchips' support (c).

References

- 1 M. Budayova-Spano, F. Dauvergne, M. Audiffren, T. Bactivelane and S. Cusack, *Acta Crystallogr., Sect. D: Biol. Crystallogr.*, 2007, **63**, 339-347.
- 2 J-P. Astier and S. Veessler, *Cryst. Growth Des.*, 2008, **8**, 4215-4219.
- 3 Š. Selimović, F. Gobeaux and S. Fraden, *Lab Chip*, 2010, **10**, 1696-1699.
- 4 J. Leng and J-B. Salmon, *Lab Chip*, 2009, **9**, 24-34.
- 5 V. Miralles, A. Huerre, F. Malloggi and M-C. Jullien, *Diagnostics*, 2013, **3**, 33-67.
- 6 P. Laval, N. Lisai, J-B. Salmon and M. Joanicot, *Lab Chip*, 2007, **7**, 829-834.
- 7 S. Teychené and B. Biscans, *Cryst. Growth Des.*, 2011, **11**, 4810-4818.
- 8 N. Junius, E. Oksanen, M. Terrien, C. Berzin, J-L. Ferrer and M. Budayova-Spano, *J. Appl. Crystallogr.*, 2016, **49**, 806-813.
- 9 H. Bruus, *Theoretical Microfluidics*, Oxford University Press, New York, 2008.